RSCPublishing

PAPER
Jaap den Toonder *et al*.
Out of the cleanroom, self-assembled magnetic artificial cilia
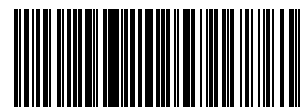
Lab on a Chip

PAPER

Out of the cleanroom, self-assembled magnetic artificial cilia†

Ye Wang,[ab] Yang Gao,[a] Hans Wyss,[a] Patrick Anderson[a] and Jaap den Toonder*[a]

Micro-sized hair-like structures, such as cilia, are abundant in nature and have various functionalities. Many efforts have been made to mimic the fluid pumping function of cilia, but most of the fabrication processes for these ''artificial cilia'' are tedious and expensive, hindering their practical application. In this paper a cost-effective *in situ* fabrication technique for artificial cilia is demonstrated. The cilia are constructed by self-assembly of micron sized magnetic beads and encapsulated with soft polymer coatings. Actuation of the cilia induces an effective fluid flow, and the cilia lengths and distribution can be adjusted by varying the magnetic bead concentration and fabrication parameters.

Introduction

In nature, microscopic hair-like structures are present in abundance. Their function may be in actuation, sensing, thermal regulation, or surface energy modification. A prominent example of these is cilia. Many water-borne micro-organisms, for example *paramecium*, use actuated cilia to propel themselves through water. The typical size of their cilia is 10–20 μm in length and hundreds of nanometers in width. The collective movement of the cilia results in very efficient swimming by the micro-organism. Also, the Fallopian tubes of a human female are covered with cilia that move the ovum. Cilia are also present in the lining of human lungs and the windpipe (trachea), to sweep mucus and dirt out of the airways in order to avoid infections. In addition to these active micro-hairs, that are used to induce movement, cilia are also used for sensing and detecting physical and chemical signals. For example immotile cilia in the cochlea, the inner ear, contribute to the detection of vibrations caused by sound. Both motile and non-motile micro-hairs are present in the human body at various locations and with various functions.[1] Apart from cilia, other types of micro-hairs are also found to be useful in nature. For example flies have hairy pads that allow them to cling to walls and ceilings,[2] while water striders have micro-hair covered legs that allow them to travel on water.[3]

The functionalities possessed by biological micro-hairs are required also in many man-made technological applications. One example is the manipulation of tiny amounts of liquids in micro-fluidic lab on a chip devices for chemical or biomedical analysis or synthesis.[4] Another is sensing: acoustic detection,[5] the detection of chemicals in the environment, or the detection of biomolecules in a miniaturized biosensor system. The active or passive surface energy modification of surfaces is also an interesting application enabling, for example, self-cleaning surfaces or self-assembly based on surface tension patterning.[6,7]

Various efforts have been made to develop micro actuators that mimic natural cilia and flagella movements.[4] Toonder *et al.*[8] fabricated micro beams with a feature size of 100 μm × 20 μm × 1 μm (length × width × thickness) from bilayer films of polyimide and chromium on the surface of ITO glass using micro-systems technologies, the beam arrays showed substantial mixing and pumping abilities when actuated electrostatically, generating a translational fluid flow rate of over 500 μm s^{-1}. Vilfan *et al.*[9] reported forming magnetic microspheres into chains by assembling them on top of pre-patterned nickel dots with optical tweezers or shape matching trenches. They actuated these chains using an external magnetic field, performing a tilted conical motion resembling the movement of embryonic nodal cilia,[10] which resulted in a net fluid flow of a few micrometers per second. The chains were 4.5 μm wide and had an aspect ratio of about 7. Evans *et al.*[11] reported the use of track-etched polycarbonate membranes as templates from which to make polydimethylsi-loxane (PDMS) micro and nanorods with embedded super-paramagnetic nanoparticles. The rods were 20 μm long and from 200 nm to 3 μm wide, depending on the hole size in the membrane. Later, these cilia were integrated into microfluidic channels by Shields *et al.*[12] and they actuated the cilia with a similar motion to Vilfan *et al.*[9] using a rotating magnet. They observed two different flow regimes, namely a translational flow above the cilia tips and a so called enhanced mixing regime below the tips. Fahrni *et al.*[13] made ferromagnetic PDMS flaps, with dimensions of 300 μm × 100 μm × 15 μm (length × width × thickness), using photolithography

[a]Department of Mechanical Engineering, Eindhoven University of Technology, Den Dolech 2, 5600 MB Eindhoven, The Netherlands. E-mail: J.M.J.d.Toonder@tue.nl
[b]Dutch Polymer Institute DPI, P.O. Box 902, 5600 AX Eindhoven, The Netherlands
† Electronic supplementary information (ESI) available: Mov Fig. 4c, Mov Fig. 5a, Mov Fig. 6a–d, Mov Fig. 6e–f. See DOI: 10.1039/c3lc50458a

techniques and actuated them externally using an electromagnetic setup, with a frequency up to 50 Hz. Rotational as well as translational flow was created with instantaneous fluid velocities of up to 500 μm s^{-1}. Other flap-like cilia with smaller dimensions (50 to 100 μm long and 10 to 20 μm wide) were made by Belardi et al.[14] using poly(n-butyl acrylate) rubber doped with nanosized superparamagnetic Fe_3O_4 particles. These cilia were integrated into a microchannel[15] and could generate a net flow of up to hundreds of micrometers per second when actuated using a rotating permanent magnet.[16] Artificial flagella, in the form of magnetic beads connected using DNA strands as linkers, were created and attached to a red blood cell by Dreyfus et al.[17] In an oscillating magnetic field the flagella performed a wave-like motion and could propel the red blood cell through liquid at 1 to 5 μm s^{-1}. The direction and speed of the propulsion could be adjusted by changing the field direction and oscillation frequency. Besides being magnetically actuatable, other types of artificial cilia have been made to show response to light,[18] pH[19] and mechanical resonance.[20]

These previous reports of artificial cilia/flagella used various methods of actuation and many of them have demonstrated the ability to generate pumping and/or mixing in a fluid environment. However, a big disadvantage of all approaches taken up until this point is that the fabrication techniques are too tedious and costly for the production of real-life products. They either require micro-system techniques like photolithography,[8,9,13–15] or have low reproducibility due to lack of control in fabrication,[17] or the fabrication processes are labor intensive and time consuming.[9,11,12]

The objective of this work is to develop a cost and time efficient, out of the cleanroom method for making magnetically actuated artificial cilia which are able to generate net flow. Superparamagnetic beads are self-assembled in an aqueous environment by an external magnetic field to form the backbone of artificial cilia. Soft polymer latex nanoparticles are adsorbed onto the surface of these beads via electrostatic attraction and form a soft coating which provides elastic links between the beads as well as an anchor to the substrate. Artificial cilia made in this way can be introduced into microfluidic devices in a straightforward manner, and not only show potential for effective fluid manipulation, but also open up other applications that can benefit from the versatile functions of natural cilia.

Construction of artificial cilia

Magnetic chains and soft polymer coating

The fabrication process is shown in Fig. 1. Artificial cilia were constructed by self-assembling magnetic beads (MBs) (Dynabeads® M-270 Carboxylic Acid, diameter 2.7 μm, 2 × 10^9 beads mL^{-1}, Invitrogen) into chains in an external magnetic field, perpendicular to the substrate. Then a layer of soft polymer was coated on the surface of the MBs and the substrate, stabilizing the shape while providing the flexibility
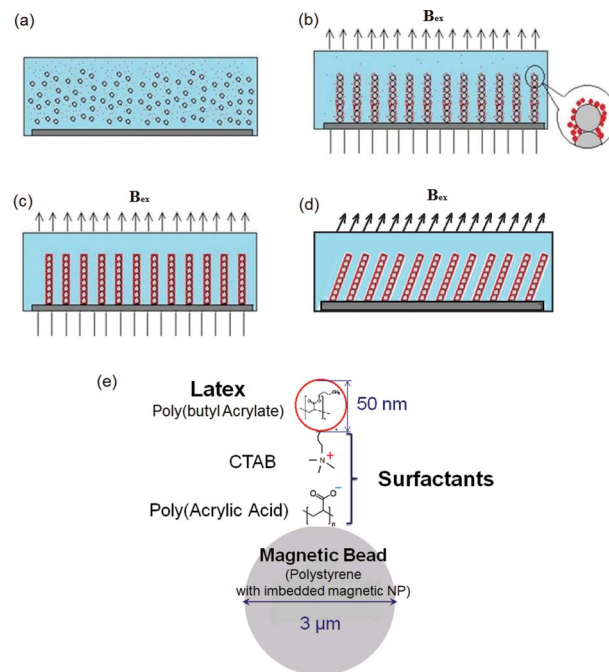
Fig. 1 Fabrication of artificial cilia. (a–d) The process of making artificial cilia in our study. First (a) a mixture of 2.7 μm spherical magnetic beads (MBs) and PBA latex is placed in a fluid cell. The black circles are MBs and red dots are poly(butyl acrylate) (PBA) latex nanoparticles. Then (b) MBs are linked into chains and attached to the surface in the presence of an external magnetic field B_{ex}. Meanwhile (b) and (c), latex particles attach to the beads by electrostatic attraction and form a continuous layer around the chains after heating. Finally (d), the enclosing PBA layer is formed and the artificial cilia can be actuated by an external field. (e) Illustration of the electrostatic adsorption of the latex on the MBs. Cetyl trimethylammonium bromide (CTAB) was used as the emulsifier in the emulsion polymerization of the PBA latex, which produced positively charged PBA nanoparticles. Poly(acrylic acid) coated MBs were chosen to provide negatively charged surfaces for electrostatic adsorption of PBA latex.

required for effective actuation. The precursor used for creating the coatings used in this study was a poly(butyl acrylate) (PBA) nanoparticle latex. The low elastic modulus and low glass transition temperature (T_g = −49 °C) of PBA facilitated the flexibility of the resulting cilia as well as the processability in aqueous environment, as a moderate heating temperature can be applied in order to accelerate the coating process.

Electrostatic attraction was used to promote adhesion between magnetic beads and PBA nanoparticles. This was achieved by using negatively charged MBs which were coated with the anionic polyelectrolyte poly(acrylic acid), and positively charged PBA latex nanoparticles which were synthesized by emulsion polymerization using a cationic surfactant cetyl trimethylammonium bromide (CTAB) as an emulsifier, shown in Fig. 1(e).

Magnetic setup for fabrication and actuation

A current driven, eight pole electromagnetic setup was previously developed in our group,[21] and is shown in the schematic in Fig. 2. With the advantage of individual control
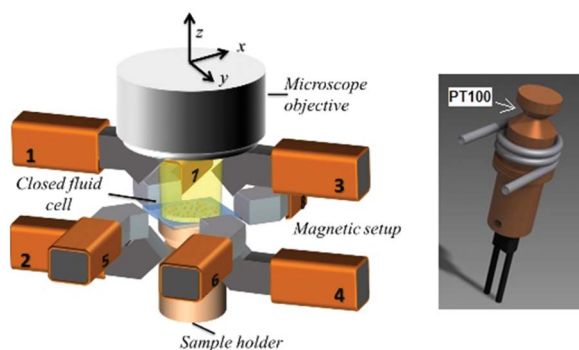
Fig. 2 Left: Schematic of the eight pole electromagnetic setup. Right: Heating/cooling sample holder, heated by a 20 W incandescent light bulb inside (not visible; only the connecting pins can be seen) and cooled by circulating coolant pumped through the wound tube. The temperature is monitored by a Pt100 thermosensor attached 3 mm below the top plane and regulated by an external temperature control unit.

Fig. 3 SEM images of the magnetic beads (2.7 μm) coated with latex. (a) Pure magnetic beads; (b) magnetic beads coated with PBA latex, washed and dried in a vacuum. Washing is performed by collecting the beads with a magnet and flushing three times with deionized water. The scale bars are 5 μm.

over each pole using a Labview® based computer program, it offers great flexibility in generating arbitrarily oriented and periodically changing magnetic fields. Fluid cells made from two 10 mm round glass coverslips separated by a double-sided adhesive spacer (Grace™ Bio-Labs SecureSeal™ imaging spacer, Sigma-Aldrich®) were used as chambers for fabrication of artificial cilia. The spacing between the two coverslips was determined by the height of the spacer as 120 ± 5 μm. After introducing the prepared mixture (see below), the cell was closed and sealed around the edge using silicone grease to prevent leakage. A temperature control element made from non-magnetic materials in the center of the setup acts as sample holder which can heat/cool the fluid cell.

In a typical fabrication process, we activate the bottom two poles (2 and 4 in Fig. 2) to apply a vertical field of 4–8 mT with a downward gradient of ~0.2 mT mm^{-1}.[21,22] The beads self-assemble into vertically oriented chains and 'stand' on the bottom surface. After the MBs are assembled, the fluid cell is heated to 40 °C in order to accelerate the process of coating the PBA latex nanoparticles on the MBs, as well as sinter the coated latex nanoparticles into a continuous layer attached to the surface of the MBs. The fluid cell was then cooled to 20 °C after 20 min. For better 'capturing' of the latex nanoparticles, a high frequency (>10 Hz) conical movement of the chains with a small rotation angle (<10°) is also applied during the fabrication process, in order to induce some mixing and increase the contact probability between the latex and the MBs. The movement was achieved by periodically actuating the four horizontal side poles (5,6,7,8 in Fig. 2) in a sinusoidal waveform input with a 90° phase lag between adjacent poles whilst maintaining a static vertical field.

Materials and methods

PBA nanoparticle latex was prepared by emulsion polymerization in the following steps: (1) 12.5 g butyl acrylate (Sigma-Aldrich) and 0.25 g CTAB were dissolved in 140 mL of deionized water in a double jacket glass reactor; (2) after nitrogen degassing for 30 min, 10 mL of 0.2 wt% potassium persulfate (KPS) solution was injected into the mixture with a
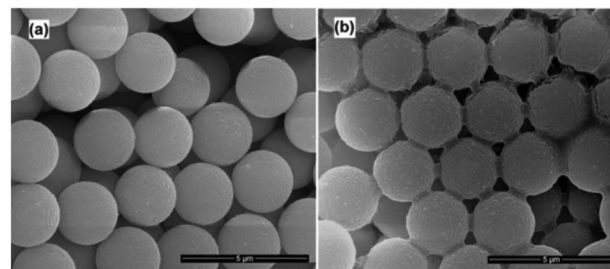
syringe, the mixture was kept at 60 °C with 500 rpm mechanical stirring during the reaction; (3) the product was collected after 12 h and dialyzed (deionized water as buffer, sample to buffer ratio 1 : 100) for 48 h at 20 °C with 500 rpm stirring, then stored at 4 °C before use.

An average size of 47 nm with a narrow distribution (Polydispersity Index 0.075) was measured for the latex particles. Zeta-potentials of latex, MBs and latex coated MBs (see below for coating procedure) were measured to be 58.8, −49 and 13.6 mV, respectively, meaning that electrostatic attraction took place and the surface charges were neutralized when the MBs and latex were mixed together. SEM photos of MBs with and without latex confirmed that a layer of PBA was coated onto the beads and connections between adjacent beads were made. Heating of the coated beads resulted in a more condensed PBA layer, while the connections remained (Fig. 3).

Particle sizes and zeta potentials were measured using a Malvern Zetasizer Nano Z with samples diluted 100 times in air equilibrated deionized water. Samples of latex coated beads for zeta potential measurement and SEM were prepared as follows: 20 μL of 1 : 1 volume ratio MB/latex mixture was diluted 100 times in deionized water, then after vortex mixing for 10 min the mixture was subjected to 2000 rpm centrifugation for 1 min, the precipitates were collected and redispersed in 2 mL of air equilibrated deionized water. SEM measurements were performed using an FEI™ Quanta™ 600 and the samples were gold coated before measurement.

The following mixture was prepared and put into the fluid cell for fabrication of artificial cilia: 10 to 20 μL MBs suspension (2 × 10^9 beads mL^{-1}, volume is varied intentionally to adjust cilia configuration, see below), 10 μL PBA latex, 20 μL 0.14 M NaCl solution, 1 μL 1 wt% Triton X-100 (Sigma-Aldrich®) and 80 μL deionized water were put in a microcentrifuge tube and mixed for 1 min on a vortex mixer to give a homogenous suspension. As a result the mixture had an overall MB concentration between 1.7 × 10^8 and 3.1 × 10^8 beads mL^{-1}. Then 8.5 μL of the mixture was placed in the fluid cell which was sonicated for a few seconds to achieve better dispersion before putting it into the magnetic setup.

Actuation and characterization

Actuation and achieving net flow

First, we calculated the local Reynolds number at the cilia tips, Re = $\rho v L/\mu$, for typical conditions in our experiments. ρ is the density of the mixture (~ 1 g mL^{-1}); v is defined as the velocity of the cilia tip which, at a typical actuation frequency of 10 Hz, is ~ 500 μm s^{-1}; L is the typical cilia length (~ 20 μm); μ is the viscosity of the mixture, which is ~ 1 cP. The calculation gives a Reynolds number of 0.01, which indicates that inertial effects do not play a role. Thus only through non-reciprocal movement can cilia generate an effective net flow.

There are two ways to actuate magnetic artificial cilia, namely through a translational force induced by a magnetic field gradient or by magnetic torque that tends to keep the chains aligned with the magnetic field. Since the artificial cilia are very small, the local field gradients are not sufficient for high frequency actuation. Instead, the torque generated by magnetic dipole–dipole interactions between magnetic beads can be very strong compared to the gradient force, due to different scaling behaviors, as explained by Fahrni et al.[13,23] Thus changing the field direction of a uniform magnetic field is our chosen method of actuation, rather than generating field gradients. In this study we used a tilted conical movement (peddling movement)[24] as illustrated in Fig. 4. This motion also occurs as so called Posteriorly Tilted Rotation-Like Beating in embryonic nodal cilia, discovered by Okada et al.[10]

A net translational flow was successfully generated by magnetic actuation (Fig. 5). Visualization of the fluid flow was achieved by adding 1.0 μm (1.0 × 10^9 beads mL^{-1}) fluorescent particles (Fluospheres® F-13081) into the fluid cell. The motion of the particles was recorded with a Leica DFC 425C CMOS-camera and later analyzed with custom written software. As shown in Fig. 5a, at the plane just above the tips of cilia (approximately 40 μm above the bottom substrate), under an actuation frequency of 1 Hz, we can see a coil like step-by-step advancing curve made by fluorescent tracer particles as they undergo a net movement towards the bottom right, which corresponds to the y direction shown in Fig. 4.

We have also observed, see Fig. 5b, that as the actuation frequency increases, the translational velocity increases in the low frequency range but decreases when the frequency is higher than 5 Hz. The explanation might be that the faster cilia movement at higher actuation frequency results in a higher viscous drag from the surrounding fluid. Indeed we have observed a reduction in the amplitude of the conical motion with an increase in the actuation frequency, which means a decrease in the half conical angle Ψ. Therefore a decrease in flow velocity is expected according to the prediction made by Smith et al.[25], that the flow velocity is proportional to $\sin^2 \Psi \sin \Theta$. A more sophisticated study into this matter is possible but it is beyond the scope of this paper. We also compared the translational velocity of the tracer particles in horizontal planes at various heights in the chamber and the result depicted in Fig. 5c shows a decrease in velocity as the focal plane moves from the tips of artificial
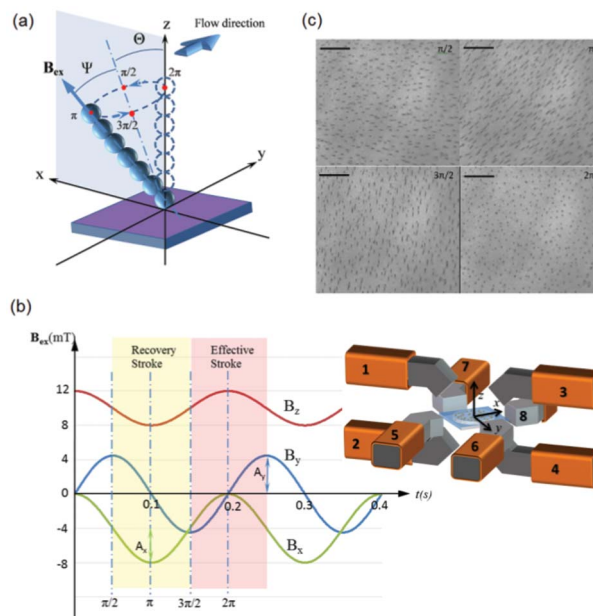
Fig. 4 Actuation of artificial cilia to generate net flow. (a) Example of the tilted conical movement of artificial cilia. In this particular case the tilt angle Θ is the same as the half-cone angle Ψ. The movement starts from an upright position perpendicular to the xy plane and follows the direction of the periodically changing external magnetic field $\boldsymbol{B}_{ex}$. The cone is tilted in the direction of the x axis. (b) The magnitude of the three components of the external field $\boldsymbol{B}_{ex}$ ($\boldsymbol{B}_x$, $\boldsymbol{B}_y$ and $\boldsymbol{B}_z$) oscillate as function of time with an actuation frequency of 5 Hz. $\boldsymbol{B}_x$ is generated by poles 5 and 8; $\boldsymbol{B}_y$ is generated by poles 6 and 7; $\boldsymbol{B}_z$ is generated by poles 1, 2, 3 and 4. In all our experiments $\Theta = \Psi = 22.5°$. The ratio of the amplitudes in the x and y directions are $A_y = A_x/\cos \theta = A_x/\cos 22.5°$, and in the z direction, the magnetic field is composed of a static part $A_{z,sta} = 2A_x(1 + \tan \theta)$, and an oscillating part with an amplitude of $A_z = A_x\tan \theta$, so that the tip of the chain follows a circular movement within the plane perpendicular to the conical axis. (C) Top-down views using the microscope with four equally divided time intervals in one actuation cycle corresponding to the external field in (B). The scale bars are 100 μm. A movie of the cilia motion is included in the ESI (Mov Fig. 4c).†

cilia towards the top of the fluid cell, with a little back flow close to the top.

We observed an effective fluid transportation effect (maximum flow velocity close to 5 μm s^{-1}) that is comparable to other reports using a similar geometry and movement of artificial cilia.[9,12] A great advantage of our approach is that by eliminating the use of micro fabrication techniques, the cost and time required for fabrication are significantly reduced. Meanwhile, being an in situ fabrication process, the method has the potential to 'plant' stable artificial cilia into existing microfluidic channels by injecting premixed building materials and applying an external magnetic field.

Dimensional stability

The polymer coatings rendered the cilia both flexible and structurally stable. Fig. 6 shows that the linear shape of the cilia is conserved without any external magnetic field, which is one of the major advantages in our approach compared with the methods of Vilfan et al.[9], who also used the self-assembling ability of magnetic beads to construct cilia, but
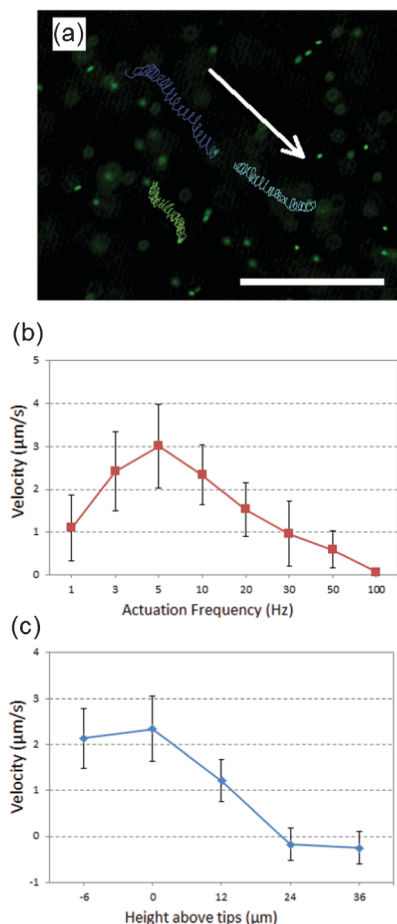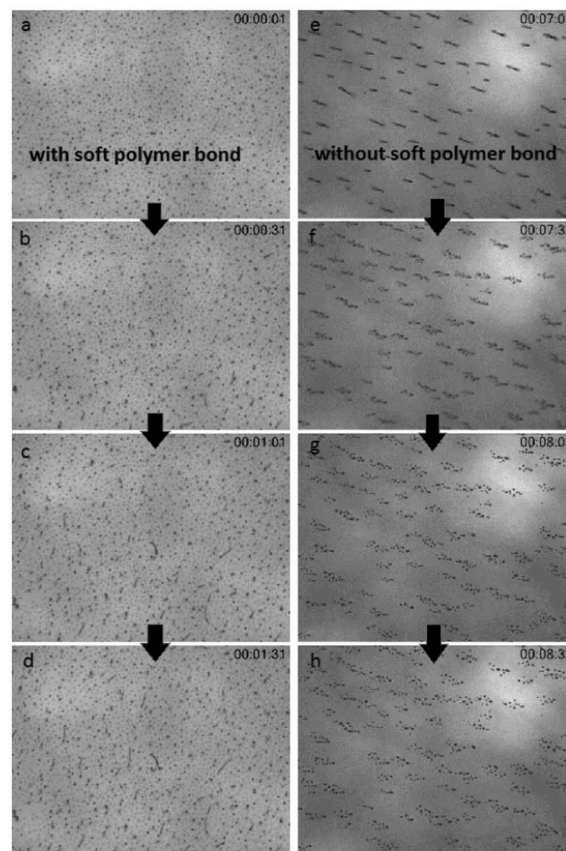
Fig. 5 Translational flow induced by artificial cilia. (a) Traces of 1 μm polystyrene fluorescent particles in the horizontal plane, 40 μm above the bottom substrate, viewed over a 20 s period with an actuation frequency of 1 Hz. Particles show a net movement towards the right bottom corner, which is the direction of the y axis in Fig. 4. The tracers also followed the circular movement of the cilia tips, so that in combination they followed a step-by-step advancing curve. The scale bar is 100 μm. A movie of the time evolution of the traces is included in the ESI (Mov Fig. 5a).† (b) Average velocities of tracer particles under different actuation frequencies, calculated using an image analysis software developed in-house. In the low frequency range (<5 Hz) the tracer velocity increases with the actuation frequency, however, the velocity decreases at higher frequencies. See more detailed discussion in the text. (c) Average velocities of tracer particles at different heights above the cilia tips at an actuation frequency of 1 Hz. It shows that as the focal plane moves up above the cilia tips a decrease in flow velocity can be observed. In both (b) and (c) the error bars are the standard deviations in the velocities of the tracer particles from a 640 μm × 480 μm frame.

Fig. 6 Structural stability of artificial cilia. (a–d) Consecutive images showing the structural stability of artificial cilia with the external magnetic field switched off. Long cilia showed bending and/or falling over time under the influence of gravity after removal of the external magnetic field; the time between each image is 30 s. The deviation in the length of cilia can be observed and all the cilia kept their structural integrity (linear shape) in the absence of the external magnetic field. (e–h) Snapshots from a comparison experiment in which the beads were not fully bonded together (insufficient latex was added); the cilia fell apart and the magnetic beads re-dispersed after the external field was switched off; time interval is 30 s. Full videos are available as ESI (Mov Fig. 6a–d and Mov Fig. 6e–f).†

the cilia are only connected by an externally applied magnetic field, thus they are not stable in the absence of the magnetic field which can be a disadvantage for practical applications.

Variation of cilia lengths and distribution

Although the length of the artificial cilia fabricated in the self-assembly process shows variation, the average length and density of artificial cilia can be controlled by varying the concentration of MBs or changing the strength of the applied magnetic field. Note that changing the cilia length also influences the density of cilia surface coverage, as more beads

are used in constructing each individual cilium. As a result we can control the average length and surface coverage of the artificial cilia within a certain range, see Fig. 7. Generally the average aspect ratio of the cilia (the average number of beads in each cilium) can vary between 5 and 20, and the surface coverage between 0.8% and 3%.

Conclusion

We have made magnetically actuated artificial cilia using a novel fabrication method. Magnetic beads were assembled into chains in an external magnetic field and a soft polymer latex was used to form elastic links between the beads through electrostatic attraction. We are able to adjust cilia density as well as their average length by varying the amount of beads and changing the external magnetic field strength during fabrication. Our cilia have a fixed width of 3 μm, determined
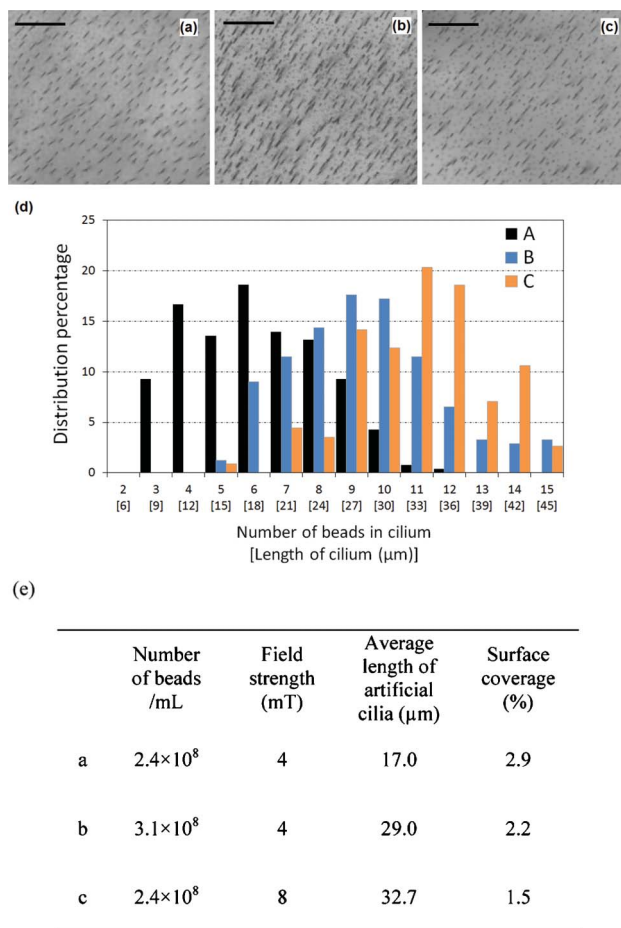
Fig. 7 Controllable average cilia length and distribution. (a–c) Top-down views of artificial cilia in different length configurations resulting from different fabrication conditions. (d) Distribution of the lengths of cilia in (a–c). (e) Differing mixture compositions and field strengths in fabrication of (a–c). Measurements were carried out by analyzing projected lengths using ImageJ and then converting to true lengths according to the angle between the cilia and the substrate, which was ~30° in (a–c). A few very long cilia were calculated to be 45 μm because of the restricted depth of focus. Surface coverage was calculated by assuming each cilium occupied the area of one bead.

by the bead size, and their aspect ratio can be as large as 11 whilst having a surface coverage of over 2%. The artificial cilia were actuated to move in a non-reciprocal manner and a net flow velocity of 3 μm s^{-1} was achieved at an actuation frequency of 5 Hz. Our result is comparable to those of other reports on actuating artificial cilia with similar geometries using the same actuation movement. There are several advantages to our approach compared to previous studies. First the fabrication process is cost and time efficient, without the need for tedious microfabrication technologies which hinder practical application. Second, the magnetic self-assembly process combined with latex coating makes a stable structure after heating which remains intact in the absence of an external magnetic field. Third, this water based assembly approach provides the possibility of *in situ* fabrication of artificial cilia in existing microfluidic devices, which enables

its use as an additional standardized, modular process for integrating artificial cilia into devices, without the necessity to modify the fabrication process of the microfluidic devices themselves. Future work will consist of studying the anchoring strength with polymeric materials such as polystyrene and polydimethylsiloxane which are commonly used in microfluidic applications, as well as studying integration with microfluidic devices and exploration of other possible functionalities of our artificial cilia.

Acknowledgements

References

1 I. Ibanez-Tallon, N. Heintz and H. Omran, *Hum. Mol. Genet.*, 2003, **12**, R27–R35.
2 E. Arzt, S. Gorb and R. Spolenak, *Proc. Natl. Acad. Sci. U. S. A.*, 2003, **100**, 10603–10606.
3 X. F. Gao and L. Jiang, *Nature*, 2004, **432**, 36–36.
4 J. M. J. den Toonder and P. R. Onck, *Trends Biotechnol.*, 2013, **31**, 85–91.
5 P. D. McGary, L. W. Tan, J. Zou, B. J. H. Stadler, P. R. Downey and A. B. Flatau, *J. Appl. Phys.*, 2006, 99.
6 T. L. Sun, L. Feng, X. F. Gao and L. Jiang, *Acc. Chem. Res.*, 2005, **38**, 644–652.
7 B. Pokroy, S. H. Kang, L. Mahadevan and J. Aizenberg, *Science*, 2009, **323**, 237–240.
8 J. den Toonder, F. Bos, D. Broer, L. Filippini, M. Gillies, J. de Goede, T. Mol, M. Reijme, W. Talen, H. Wilderbeek, V. Khatavkar and P. Anderson, *Lab Chip*, 2008, **8**, 533–541.
9 M. Vilfan, A. Potocnik, B. Kavcic, N. Osterman, I. Poberaj, A. Vilfan and D. Babic, *Proc. Natl. Acad. Sci. U. S. A.*, 2010, **107**, 1844–1847.
10 Y. Okada, S. Takeda, Y. Tanaka, J. C. I. Belmonte and N. Hirokawa, *Cell*, 2005, **121**, 633–644.
11 B. A. Evans, A. R. Shields, R. L. Carroll, S. Washburn, M. R. Falvo and R. Superfine, *Nano Lett.*, 2007, **7**, 1428–1434.
12 A. R. Shields, B. L. Fiser, B. A. Evans, M. R. Falvo, S. Washburn and R. Superfine, *Proc. Natl. Acad. Sci. U. S. A.*, 2010, **107**, 15670–15675.
13 F. Fahrni, M. W. J. Prins and L. J. van IJzendoorn, *Lab Chip*, 2009, **9**, 3413–3421.
14 J. Belardi, N. Schorr, O. Prucker and J. Ruhe, *Adv. Funct. Mater.*, 2011, **21**, 3314–3320.
15 S. N. Khaderi, C. B. Craus, J. Hussong, N. Schorr, J. Belardi, J. Westerweel, O. Prucker, J. Ruhe, J. M. J. den Toonder and P. R. Onck, *Lab Chip*, 2011, **11**, 2002–2010.
16 J. Hussong, N. Schorr, J. Belardi, O. Prucker, J. Ruhe and J. Westerweel, *Lab Chip*, 2011, **11**, 2017–2022.
17 R. Dreyfus, J. Baudry, M. L. Roper, M. Fermigier, H. A. Stone and J. Bibette, *Nature*, 2005, **437**, 862–865.

18 C. L. van Oosten, C. W. M. Bastiaansen and D. J. Broer, *Nat. Mater.*, 2009, **8**, 677–682.

19 L. D. Zarzar, P. Kim and J. Aizenberg, *Adv. Mater.*, 2011, **23**, 1442–1446.

20 K. Oh, B. Smith, S. Devasia, J. J. Riley and J. H. Chung, *Microfluid. Nanofluid.*, 2010, **9**, 645–655.

21 Y. Gao, M. A. Hulsen, T. G. Kang and J. M. J. den Toonder, *Phys. Rev. E*, 2012, 86.

22 Y. Gao, A. van Reenen, M. A. Hulsen, A. M. de Jong, M. W. J. Prins and J. M. J. den Toonder, *Lab Chip*, 2013, **13**, 1394–1401.

23 F. Fahrni, M. W. J. Prins and L. J. van IJzendoorn, *J. Magn. Magn. Mater.*, 2009, **321**, 1843–1850.

24 M. T. Downton and H. Stark, *EPL*, 2009, 85.

25 D. J. Smith, J. R. Blake and E. A. Gaffney, *J. R. Soc. Interface*, 2008, **5**, 567–573.